ACS OMEGA

Open Access

http://pubs.acs.org/journal/acsodf

Article

Comprehensive Analysis of Pressure Drop Phenomena in Rotating Packed Bed Distillation: An In-Depth Investigation

Amiza Surmi, Azmi Mohd Shariff,* and Serene Sow Mun Lock

Cite This: *ACS Omega* 2024, 9, 28105−28113

Read Online

ACCESS | Metrics & More | Article Recommendations

ABSTRACT: A rotating packed bed (RPB) is an innovative intensification technology that improves its separation capabilities in high-gravity conditions. This process increases efficiency with smaller equipment size and footprint than conventional packed columns. Although significant advancements have been made regarding RPBs, most studies only focused on single or dual rotor configurations in addressing dry pressure drop. Hence, multiple rotor systems in industrial settings can enhance economic efficiency by minimizing the necessity for numerous RPBs. This study investigated the pressure drops and holdup in a three-stage rotor-based RPB under actual process conditions using natural gas as the feed. A novel pressure drop correlation was introduced based on the nitrogen removal process from the natural gas in continuous RPB distillation operations. Consequently, the correlation between centrifugal acceleration, turbulent, and momentum effects demonstrated remarkable accuracy within ±15%. This outcome also highlighted the importance of meticulous design considerations in RPB-based applications due to the complex correlation between centrifugal forces, liquid holdup, and gas flow rates. The reflux feed ratio, liquid holdup, rotating speed, and *F*-factor effects were examined to comprehend the RPB distillation process. Overall, the correlations between the critical parameters offered crucial insights to prevent process upsets (such as flooding), contributing to advancing RPBs in practical industrial settings.

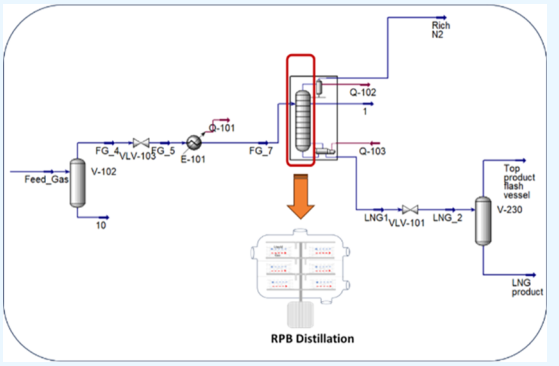

1. INTRODUCTION

The distillation column is pivotal in refining and chemical processes for separating components of a mixture based on their boiling points. Distillation is critical in achieving specific product purities and process efficiencies, accounting for a significant proportion (40−60%) of energy consumption in the industrial sectors.[1,2] The internal design of the columns involving the packing or tray configurations is instrumental in enhancing mass transfer and facilitating effective gas−liquid interactions.[3] Nonetheless, achieving high separation performance in situations requiring stringent product purity results in taller columns with more stages or packing volumes. This design can be problematic in space-constrained environments, such as brownfield projects or offshore facilities.

A study by Ramshaw and Mallinson developed the first rotating packed bed (RPB) in 1981, which was a significant advancement in process intensification to address these challenges.[4] The study revealed that this innovative technology involving high-gravity concepts improved mass transfer efficiency in distillation and absorption processes, reducing the space required for the equipment. Generally, RPBs consist of a cylindrical packing material bed rotating around a central axis. This stage generates a high-gravity environment through centrifugal force, substantially enhancing the gas−liquid interaction than traditional packed beds. A commercial-scale RPB installation by HiGee Environment and Energy Technologies, Inc. at the Fujian Refining and Petrochemical Company Ltd., China, documented that the intensified approach significantly decreased the size of separation units by 2−3 orders of magnitude.[5−7]

Figure 1 depicts that the RPB is commonly applied in absorption and desorption,[8−14] distillation,[15−19] catalytic reactions,[20,21] wastewater treatment,[22−24] and electrolysis.[25−27] Several studies have reported that increasing the rotational speed enhances the mass and heat transfer rate. Certain studies have also highlighted that the absorption process can be performed at speeds exceeding 1000 rpm.[28−30] In contrast, this process produces higher power as motor energy is proportional to the square of motor power.[31] Hence, the optimal point for the process should be identified by determining the right balance between power and efficiency.

Received: February 4, 2024
Revised: May 18, 2024
Accepted: May 28, 2024
Published: June 14, 2024

https://doi.org/10.1021/acsomega.4c01128
ACS Omega 2024, 9, 28105−28113

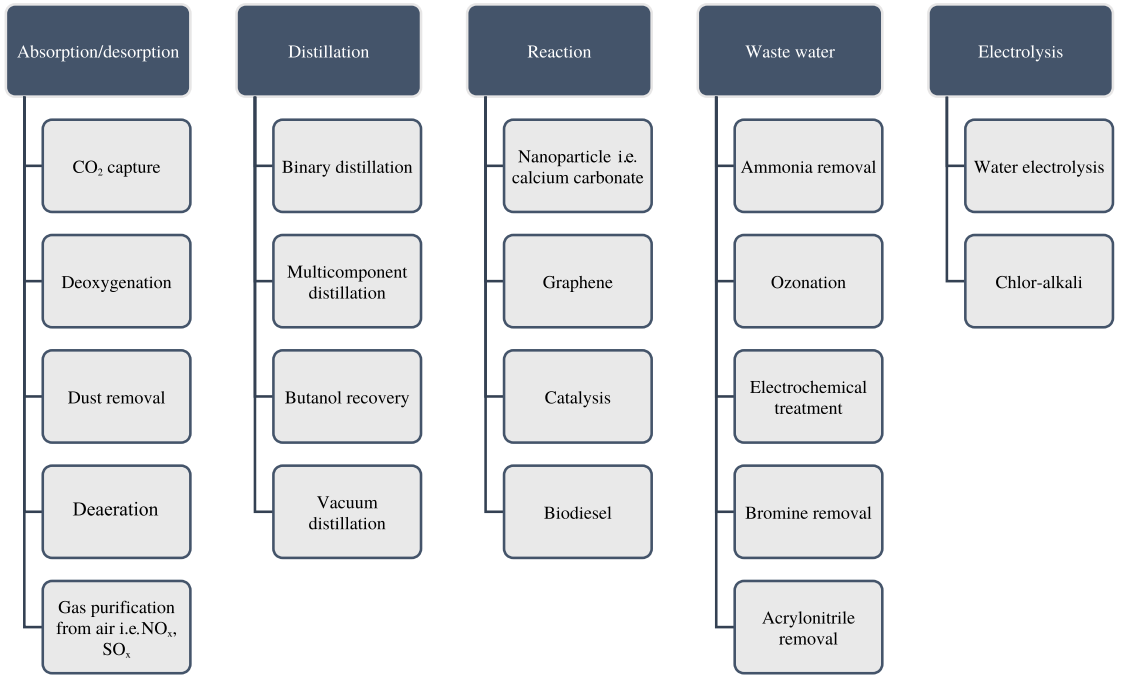

Figure 1. RPB-related research and development categories.

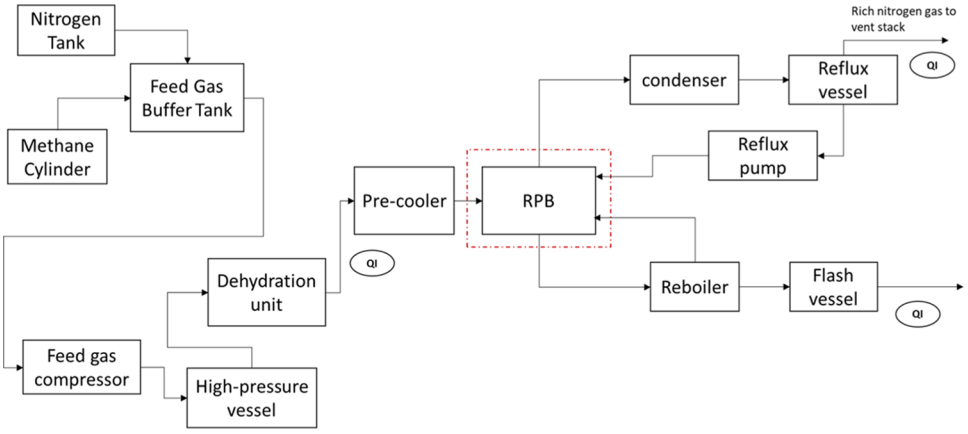

Figure 2. Block diagram for the overall test setup of the cryogenic nitrogen removal process (Cryonru).

Despite the superior mass transfer capabilities of RPBs, this system encounters difficulties with hydrodynamics and pressure drops under high centrifugal acceleration conditions. Pressure drops across components inside conventional distillation columns usually require extra equipment (such as pumps or compressors) to maintain desired flow rates and process conditions. Meanwhile, a significant pressure drop in an RPB requires higher design pressure and rotating equipment, leading to a higher cost. Since 1988, numerous studies have advanced the comprehension of pressure drops in RPBs. A study by Keyvani and Gardner achieved an early breakthrough by developing a semiempirical correlation for pressure drops with foam metal packing at different surface areas and rotational speeds.[32] The study denoted that lower pressure drops were observed in irrigated beds compared to dry ones.

Another study by Liu et al. examined the influence of packing material characteristics and gas flow rate on pressure drop. Likewise, Sandilya et al. discovered minimal pressure drop effects from the expansion and contraction in single-rotor-based RPBs.[33] Alternatively, Jiao et al. investigated the gas pressure drop in a crossflow-based RPB,[34] while Hendry et al. analyzed the pressure drop in a horizontal RPB setup using metal mesh packing.[35] Pyka et al. also conducted a recent study involving new correlations for pressure drop in dual-rotor-based RPBs from 300 to 900 rpm.[36] Similarly, Llerena-Chavez et al. used computational fluid dynamics (CFD) to assess the dry pressure drop across RPBs with a single-phase flow model while introducing a new semiempirical equation.[37] Wojtasik-Malinowska et al. also applied CFD modeling to analyze pressure drops in RPBs with porous packing to optimize the system design.[38]

Liquid holdup is a crucial parameter in the performance of an RPB, which can significantly impact the mass transfer efficiency. The liquid is propelled outward due to centrifugal acceleration, creating a thin film on the packing surface. Therefore, this process significantly affects the liquid holdup. A study by Burns et al. extensively researched the factors affecting liquid holdup and validated their model with experimental results.[39] Consequently, the study was widely utilized by other

https://doi.org/10.1021/acsomega.4c01128
ACS Omega 2024, 9, 28105−28113

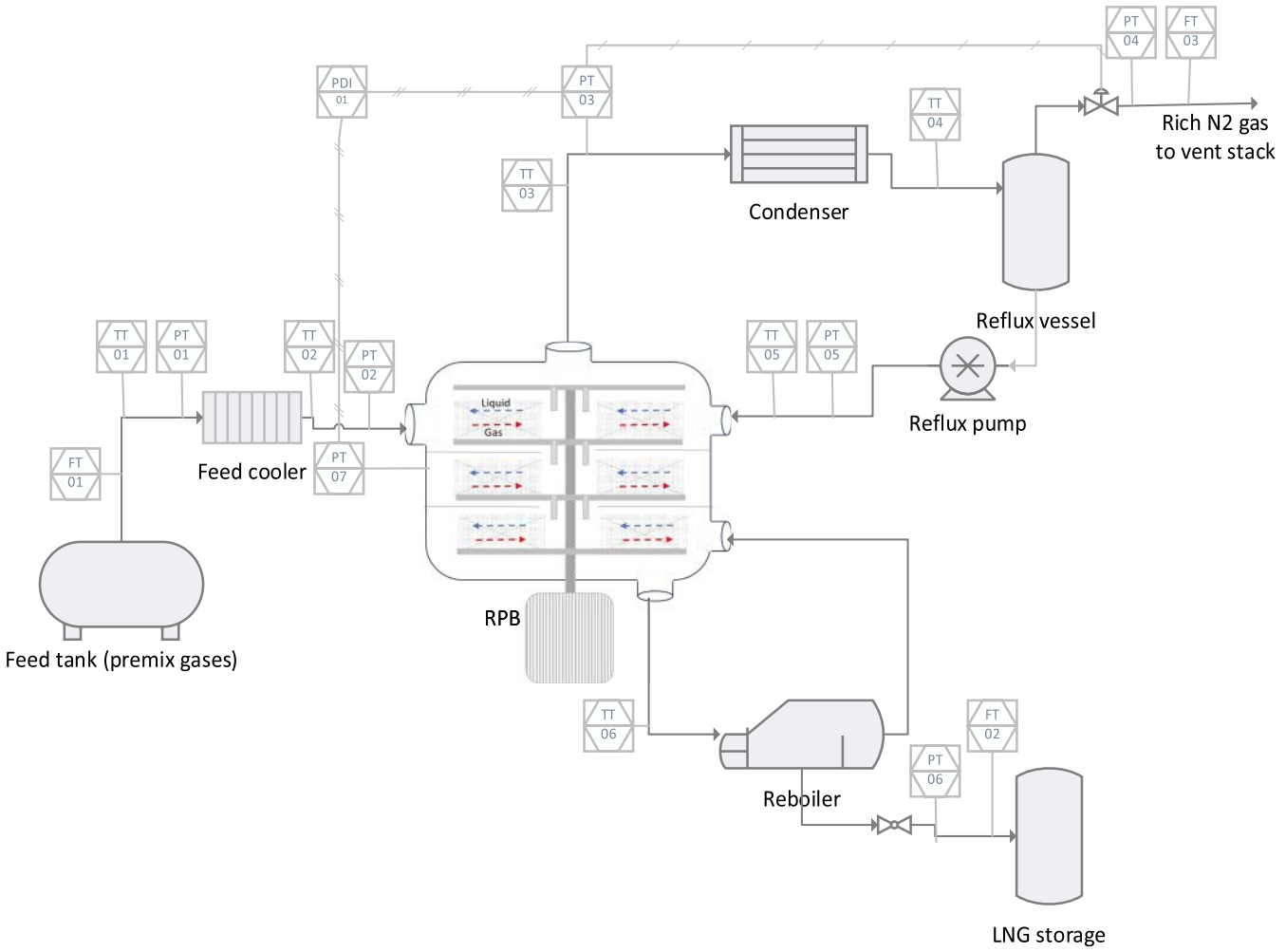

Figure 3. Cryonru process configuration for the low-temperature distillation process.

researchers.[31,39] Other studies have also pointed out the importance of liquid holdup in RPBs, demonstrating its influence on micromixing efficiency, mass transfer rates, and overall system performance.[23,40−42]

Most studies have focused on the performance of RPBs at typical operating temperatures and lower operating pressures, which frequently involve single or dual rotor stages. Nevertheless, more stages are required when the feed gas contains more contaminants or higher purity levels are desired, increasing the number of rotors. Thus, this study investigated the pressure drop across a three-stage rotor setup used to remove nitrogen from natural gas in a cryogenic process for liquefied natural gas (LNG) production.

2. MATERIALS AND METHODS

2.1. Experimental Setup. Figures 2 and 3 illustrate the high-pressure and cryogenic pilot plant employed in this study for simulating a continuous process at the Cryonru facility. The advanced system consisted of various critical components, such as molecular sieve (mol-sieve) dehydration vessels, feed coolers, a cryogenic RPB distillation unit, a condenser, a reboiler, a reflux vessel, a reflux pump, a flash vessel, and a vaporizer. This stainless steel setup was meticulously interconnected through a piping network to ensure seamless process integration.

The mass transfer experiments focused on nitrogen removal from a binary nitrogen-methane mixture. Initially, the feed gases sourced from cylinders or tanks were directed to the mol-sieve dehydration unit. In subsequent low-temperature operations, the moisture was reduced to only 0.1 ppm to avoid excessive humidity, producing hydrate formation and clogging issues. After dehydration, the gases were compressed from 10 to 40 bar and mixed to create a homogeneous blend of gases using a recycle line. This mixture was cooled to at least −130 °C using feed coolers and then subjected to a pressure reduction to 15 bar.

The Cryonru setup was designed to mimic a traditional distillation column and featured the cryogenic RPB distillation unit as its primary component. This RPB setup contained upper (condenser, reflux vessel, and reflux pump) and lower (reboiler and flash vessel) sections. The upper and lower products of both sections then produced LNG and nitrogen with minimal methane content, respectively. Moreover, the RPB, piping, and all integrated equipment were insulated with low-temperature thermal insulation materials and metal jacketing to maintain the required operating temperature while minimizing heat loss. This feature was essential to ensure that the LNG remained liquid in the LNG storage vessel.

The facility was equipped with gas chromatography (GC) and an online sampling line directly connected to the GC for real-time feed gas, nitrogen-enriched products, and LNG

https://doi.org/10.1021/acsomega.4c01128
ACS Omega 2024, 9, 28105−28113

analysis. A programmable logic controller (PLC) was also employed as an interface for the process control and instrumentation system to regulate pressure, temperature, level, and flow within the processing unit. Several variables were then systematically varied during testing, including the rotational speed of the RPB (300−900 rpm) and operational pressure (12−15 bar). The nitrogen concentration in the feed gas was also adjusted to thoroughly evaluate the nitrogen separation performance under different high-gravity conditions using cryogenic RPB distillation. Particularly, the RPB possessed wire mesh packing (0.85 porosity), diameter and height of 1 m, respectively, and variable speed control for precise operational adjustments.

2.2. Pressure Drop Analysis. This study assessed the RPB operations at pressures higher above atmospheric pressure and cryogenic temperatures, which were topics not previously addressed in previous studies. Therefore, the nitrogen removal process for producing LNG was focused on using a cryogenic experimental setup with an RPB. A critical component of the experimental procedure also involved the cooling down phase, encompassing the entire system (including the cryogenic RPB distillation). This step was carefully controlled to prevent rapid cooling, which could cause thermal expansion with potential hydrocarbon leakage at the joints and freezing issues during the low-temperature processes.

The pressure was an essential parameter in the distillation process (similar to traditional distillation methods), which ensured that the optimal condensation and reboiling rates reached the desired separation efficiency. Thus, the pressure drop across the RPB was mainly monitored as part of the experimental protocol. This pressure drop was also primarily affected by the turbulent fluid behavior, centrifugal effects from rotational accelerations, and momentum effects (described in this study using a semiempirical equation). Additionally, the pressure drop caused by the angular velocity of the rotor due to centrifugal acceleration was significant in the overall pressure dynamics of the RPB. Therefore, this discovery was supported by other studies and incorporated into the correlations of this study.

The observations indicated that the gas phase pressure drop was more pronounced than the liquid phase. This outcome was attributed to the lower liquid holdup produced by the centrifugal force, rendering the gas flow rate a more critical factor than the liquid flow rate. Thus, a new correlation was developed to account for the pressure drop caused by turbulence inside the RPB. The effects of centrifugal acceleration were also integrated into this correlation, which was regulated by a variable frequency drive to control the speed of the rotor. Considering that the momentum effect was integrated following a study by Sandilya et al.,[43] this effect was incorporated into new equations to account for the impact of solid slip between the fluid and internal packing on pressure drop. The equation for the total pressure drop (ΔP_{total}) is expressed as follows:

$$\Delta P_{total} = \Delta P_t + \Delta P_c + \Delta P_m$$

where ΔP_t is the pressure drop due to turbulence, ΔP_c is the pressure drop due to centrifugal acceleration, and ΔP_m is the pressure drop due to momentum. Hence, the equation for ΔP_t is formulated as follows:

$$\Delta P_t = \frac{1.75(1-\varepsilon)\rho}{d\varepsilon^3}\left(\frac{G}{2\pi Z}\right)^2\left(\frac{1}{r_2}-\frac{1}{r_1}\right) \quad (1)$$

Meanwhile, the ΔP_c of fluids in an RPB consisted of the rotor and internal packing. Hence, the equation for ΔP_c is expressed as follows:

$$\Delta P_c = K\int_{r_1}^{r_2}\rho_g\frac{v_0^2}{r}\mathrm{d}r = K\rho_g\int_{r_1}^{r_2} r\omega^2\mathrm{d}r = \frac{\rho_g}{2}K\omega^2(r_2^2-r_1^2) \quad (2)$$

where the value of K is determined from the regression of the experimental result (1.31529). Likewise, the equation for ΔP_m is formulated as follows:

$$\Delta P_m = \rho_g\int_{r_1}^{r_2}\frac{\bar{V}_r^2}{r}\mathrm{d}r = \frac{1}{2}\rho_g\left(\frac{Q_g}{2\pi a\epsilon}\right)^2\left(\frac{1}{r_1^2}-\frac{1}{r_2^2}\right) \quad (3)$$

Consequently, eq 1 is denoted as follows:

$$\Delta P_{total} = \frac{1.75(1-\varepsilon)\rho}{\mathrm{d}\varepsilon^3}\left(\frac{G}{2\pi Z}\right)^2\left(\frac{1}{r_2}-\frac{1}{r_1}\right) + \frac{\rho_g}{2}\omega^2(r_2^2-r_1^2) + \frac{1}{2}\rho_g\left(\frac{Q_g}{2\pi a\epsilon}\right)^2\left(\frac{1}{r_1^2}-\frac{1}{r_2^2}\right) \quad (4)$$

2.3. Error Analysis. The proposed semiempirical model is evaluated using the absolute average relative deviation percent [AARD (%)] and correlation coefficients (R^2) as follows:[44]

$$\mathrm{AARD}\ (\%) = \sum_i^n\left(\left|\frac{p_i^{exp}-p_i^{calc}}{p_i^{exp}}\right|\right)\frac{1}{n}\times 100 \quad (5)$$

$$R^2 = \frac{\sum_1^n (P_i^{exp}-\bar{p})^2 - \sum_1^n (P_i^{exp}-p_i^{calc})^2}{\sum_1^n (P_i^{exp}-\bar{p})^2} \quad (6)$$

where n denotes the number of data points from the experiment, P_i^{exp} and p_i^{calc} denote the pressure drops from the experiment and calculation, respectively, and $\bar{p}$ denotes the average pressure drop from the experiment.

3. RESULTS AND DISCUSSION

3.1. Pressure Drop. Figure 4 displays the parity plot comparing experimental and calculated pressure drops, demonstrating a close agreement within ±15% AARD and 95.5% R^2. The results validated the effectiveness of the newly

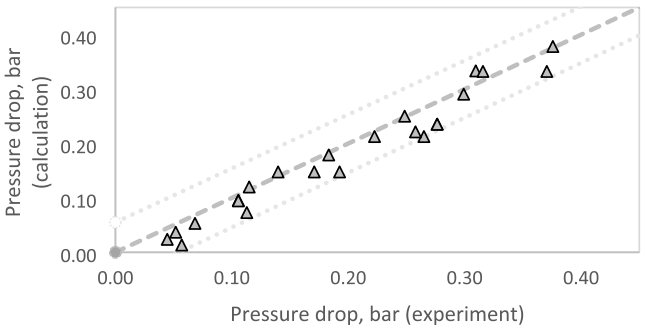

Figure 4. Parity plot for the experimental and calculated pressure drop.

https://doi.org/10.1021/acsomega.4c01128
ACS Omega 2024, 9, 28105−28113

developed correlation, which was specifically tailored for a three-stage rotor system. Thus, the proposed correlation in this study was robust in predicting pressure drops for RPBs. Figure 5 portrays that the correlation offers a more accurate forecast

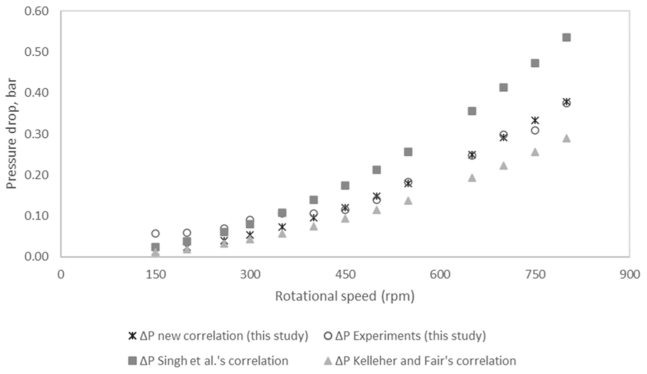

Figure 5. Pressure drop from the experimental and calculated pressure drop.

of the pressure drop across the RPB at varying rotational speed compared to the models proposed by Kelleher and Fair (see eq 7)[45] and Singh et al. (see eq 8)[46] as follows:

$$P_{\text{total}} = A'\frac{\rho_g \omega^2}{2}(r_2^2 - r_1^2) + B_1\frac{a_t}{\epsilon}\rho_g(r_2 - r_1)U_{\text{avg}}^2 \quad (7)$$

$$\Delta P = \frac{\rho_g \omega^2}{2}(r_2^2 - r_1^2) + \frac{5B'}{22}\left(\frac{\epsilon \dot{m}_g}{\pi h \rho_g}\right)^2\left(\frac{1}{r_1^{1.1}} - \frac{1}{r_2^{1.1}}\right) \quad (8)$$

This study revealed that the pressure drop increased directly to centrifugal acceleration, consistent with the correlation findings from Kelleher and Fair[45] and Singh et al.[46] All three correlations presented a strong agreement below 300 rpm. Conversely, pressure drops significantly above 600 rpm, following theoretical predictions. This study also discovered that the correlation between centrifugal and fluid friction factors within porous media in Singh et al.'s study tended to overestimate pressure drops (particularly above 500 rpm).[46] Furthermore, the difference became more pronounced at higher speeds. Alternatively, the correlation from Kelleher and Fair tended to underestimate pressure drops at rotational speeds above 350 rpm (precisely above 600 rpm).[45] The observation was based on correlations determined from cyclohexane or *n*-heptane experiments conducted under specific conditions [operating pressures = 166 and 414 kPa (total reflux conditions)].[45]

Typically, flooding in packed columns is a significant operational constraint caused by the excessive accumulation of the liquid phase. This phenomenon significantly hinders gas flow and reduces mass transfer efficiency, notably increasing the pressure drop or reducing it in a column throughput. Hence, the functionality of the column at this juncture is severely compromised, resulting in operational instability. On the contrary, flooding in RPBs presents unique challenges. This phenomenon occurs when centrifugal forces cannot distribute the liquid phase evenly, producing accumulation at the packing and the eye of the rotor. Previous studies denoted that this scenario was commonly associated with either excessive liquid presence or inadequate drainage, which was potentially due to excessive centrifugal acceleration (particularly at the eye of the rotor).[47] Consequently, the interaction between vapor and liquid was significantly obstructed, reducing separation efficiency.

Figure 6 illustrates the correlation between liquid load and pressure drop. A higher liquid load from 0.7 to 0.9 $m^3/h\ m^2$

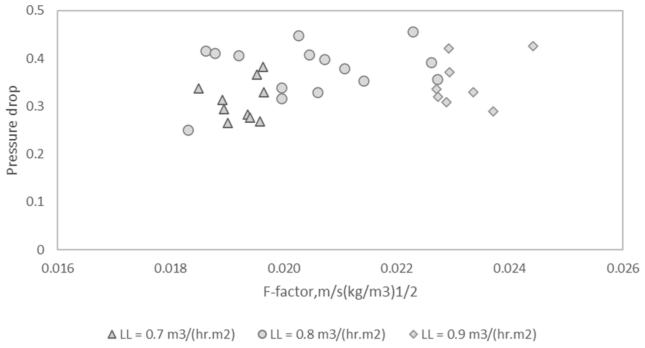

Figure 6. Effect of the F-factor on the pressure drop at different liquid loading.

demonstrated only a marginal increase in pressure drop, with a peak at approximately 0.45 bar. This outcome suggested a nonlinear correlation between liquid load and pressure drop, indicating additional factors influencing flooding (see eqs 9 and 10).[41,47]

$$\text{superficial velocity:}\quad U = \frac{Q}{A} = \frac{Q}{\pi(r_2^2 - r_1^2)} \quad (9)$$

$$F\text{-factor:}\quad F = U\sqrt{\rho} \quad (10)$$

The *F*-factor for indicating gas velocities or densities was also identified as a critical parameter. Thus, a threshold F-factor value of 1.5 m/s $(kg/m^3)^{1/2}$ observed in this study implied a high risk of flooding in the RPB. This threshold was crucial for predicting when flooding conditions could occur. Figure 7 displays how rotational speed variations affect the

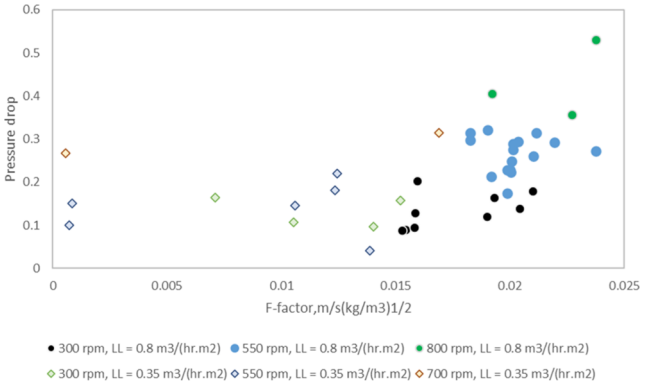

Figure 7. Effect of the rotational speed on the F-factor and pressure drop.

system, specifically at 0.35 and 0.8 $m^3/h\ m^2$ liquid loads. Consequently, a higher rotational speed (700 rpm) caused a pressure drop of less than 0.3 bar for a lower liquid load of 0.3 $m^3/h\ m^2$. When the liquid flow rate increased to 0.8 $m^3/h\ m^2$, the *F*-factor and pressure drop increased dramatically with higher rotational speed. Nevertheless, these were still lower than the predetermined threshold for this study.

https://doi.org/10.1021/acsomega.4c01128
ACS Omega 2024, 9, 28105−28113

Overall, the correlations between liquid load, rotational speed, and the *F*-factor in RPB operations were complex and significantly impacted the efficiency and stability of the system. The results enhanced comprehension of flooding dynamics in RPBs and established vital benchmarks for operational parameters to mitigate flooding risks.

3.2. Reflux Feed Ratio. This study investigated how the reflux feed ratio (RFR) in a distillation column affected separation efficiency, energy utilization, and overall column design. Figure 8 depicts a significant increase in pressure drop

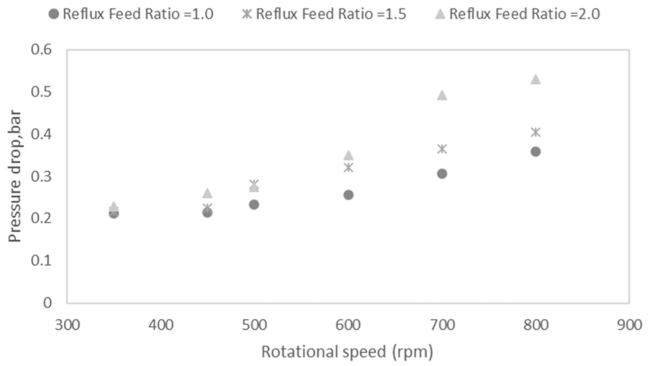

Figure 8. Effects of reflux feed ratio and rotational speed.

in the RPB as the reflux feed ratio increases. The pressure drops at a reflux feed ratio of 2 increased significantly once the rotational speed exceeded 600 rpm. This phenomenon was potentially caused by higher liquid flowing back to the RPB and the rotor eye, leading to increased turbulence at higher speeds. Specifically, the rotor eye was a crucial area for liquid−gas interaction and was prone to flooding during high liquid and intense gas−liquid traffic conditions.

A substantial risk of liquid entrainment could occur within the gas stream at high reflux feed ratios, contributing to increased pressure drops. The pressure drops highlighted minor sensitivity to reflux feed ratio variations at rotational speeds below 500 rpm. Figure 9 further elucidates the

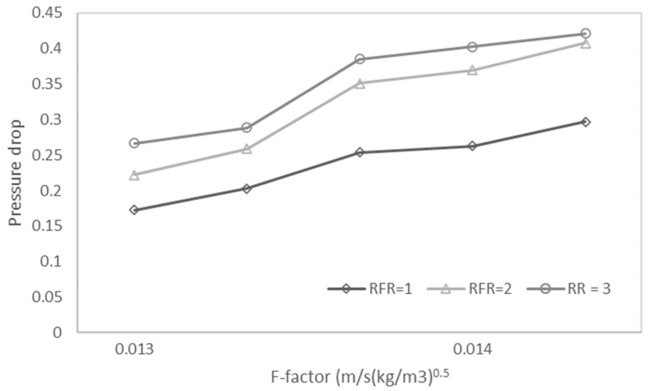

Figure 9. Effects of reflux feed ratio and *F*-factor.

correlation between *F*-factor, pressure drop, and reflux feed ratio. Consequently, increasing the reflux feed ratio from 1 to 3 significantly increased the pressure drop (particularly at lower *F*-factors). This outcome was attributed to the excessive liquid recycling and subsequent liquid entrainment in the gas phase.

The influence of the reflux feed ratio on pressure drop diminished at higher *F*-factors, suggesting a higher stabilized system behavior. Although the pressure drop at a reflux feed ratio of 1 was comparatively lower than at reflux feed ratios of 2 and 3, this pressure drop increased with a higher *F*-factor. These observations underscored the complex correlation between centrifugal acceleration and liquid−gas dynamics in the RPB, stressing the importance of a thorough study to improve rotor design for mitigating flooding risks at targeted reflux feed ratios. Therefore, attaining an optimal reflux feed ratio was crucial for distillation processes to achieve high separation efficiency.

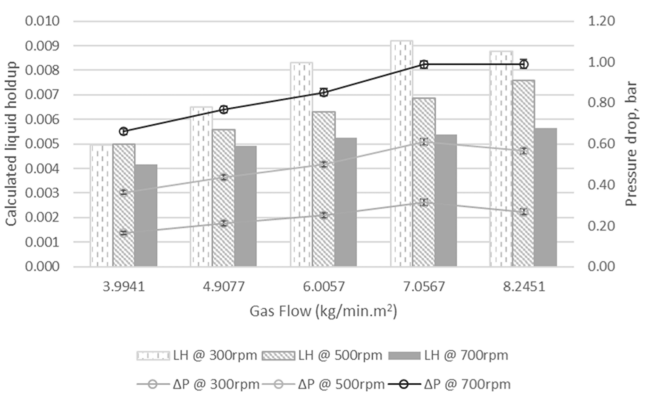

Figure 10. Effects of gas flow, liquid holdup, and pressure drop at different speeds.

3.3. Liquid Holdup. Figure 10 portrays the effect of gas flow rate, pressure drop, and calculated liquid holdup following the correlation reported by Burns et al. as follows:[39]

$$\varepsilon_L = 0.034\left(\frac{g}{g_0}\right)^{-0.38}\left(\frac{U}{U_0}\right)^{0.62} \quad (11)$$

where g_0 = 100 m/s^2 and U_0 = 1 cm/s. The pressure drop and liquid holdup became lower when the rotational speed increased from 300 to 700 rpm at the constant gas flow rate, which was in agreement with previous studies.[48,49] Meanwhile, a 3.9941 kg/min gas flow rate at 300 rpm produced a minimal pressure drop of 0.2 bar and liquid holdup of 0.005. Conversely, a significant increase in the pressure drop (1.08 bar) and liquid holdup (0.0088) was recorded when the gas flow rate increased to 7.0567 kg/min. This finding was potentially due to small liquid entrainment in the gas stream as the flow rate and rotational speed increased.

A higher gas flow rate of 8.2 kg/min slightly reduced the pressure drop and liquid holdup. This outcome was attributed to stabilizing the rotation within the rotor packing, resulting in reduced turbulence and liquid entrainment in the gas outlet stream. On the contrary, increasing the rotational speed to 700 rpm gradually raised pressure drop and liquid holdup with only marginal increments. This phenomenon could be caused by higher liquid entrainment in the gas stream at higher liquid holdup and gas flow rates, contributing to a higher pressure drop. An increase in rotation speed from 300 to 700 rpm at a constant gas flow rate of 4 kg/min also resulted in lower liquid holdup and pressure drop (specifically at 6 to 7 kg/min gas flow rate). This observation indicated that improved gas−liquid contact promoted better interaction between gas and liquid phases, reducing pressure drop and liquid holdup.

https://doi.org/10.1021/acsomega.4c01128
ACS Omega 2024, 9, 28105−28113

Overall, the flood limit should be avoided to prevent turbulent conditions within the RPB from affecting separation efficiency. The results highlighted the importance of careful design considerations in RPB applications due to the complex interplay of centrifugal forces, liquid holdup, and gas flow rates. Therefore, finding this equilibrium was crucial for maximizing the capabilities of RPB in separation processes to achieve better efficiency.

4. CONCLUSIONS

The study entailed the construction of a cryogenic pilot facility that utilized a low-temperature RPB distillation system to extract liquefied natural gas (LNG) at a minimum temperature of −161 °C and a maximum pressure of 15 bar. A 15% increase in accuracy was attained during the formulation of novel pressure drop correlations that accounted for momentum, centrifugal acceleration, and turbulence. Liquid holdup was found to be diminished with increased rpm, while pressure drop and holdup were found to be positively correlated with gas flow rate. This results in liquid interaction in the RPB. Moreover, fluctuations in the reflux feed ratio were noted in this investigation, which led to the conclusion that an escalation in rotational velocity is commensurate with an increase in pressure drop. This increase became significant when the rotational speed exceeded 600 rpm at a 2.0 reflux feed ratio. As a consequence of the subsequent escalation in flooding risk brought about by the rotor's excessive liquid levels, nitrogen removal efficiency was diminished. However, the F-factor results provided evidence that the potential for flooding was significantly reduced compared to the threshold. For industrial applications in particular, additional research is necessary to determine the upper and lower flooding limits of low-temperature RPB distillation.

AUTHOR INFORMATION

Corresponding Author

Azmi Mohd Shariff − *Chemical Engineering Department, Universiti Teknologi PETRONAS, 32610 Seri Iskandar, Perak, Malaysia; CO_2 Research Center, Universiti Teknologi PETRONAS, 32610 Seri Iskandar, Perak, Malaysia;* orcid.org/0000-0001-8524-1994; Email: azmish@utp.edu.my

Authors

Amiza Surmi − *Chemical Engineering Department, Universiti Teknologi PETRONAS, 32610 Seri Iskandar, Perak, Malaysia; Group Research & Technology, Petroliam Nasional Berhad (PETRONAS), Kawasan Institusi Bangi, 43000 Kajang, Selangor, Malaysia;* orcid.org/0009-0005-8071-3602

Serene Sow Mun Lock − *Chemical Engineering Department, Universiti Teknologi PETRONAS, 32610 Seri Iskandar, Perak, Malaysia; CO_2 Research Center, Universiti Teknologi PETRONAS, 32610 Seri Iskandar, Perak, Malaysia;* orcid.org/0000-0003-2285-0308

Complete contact information is available at: https://pubs.acs.org/10.1021/acsomega.4c01128

Funding

This research was funded by PETRONAS Research Sdn Bhd, Grant Numbers 015MD0-055, 015MD0-126, and 015MD0-089, and Yayasan Universiti Teknologi PETRONAS, Grant Number 015LC0-390.

Notes

The authors declare no competing financial interest.

ACKNOWLEDGMENTS

The authors acknowledge the cost centers 015MD0-055, 015MD0-126, and 015LC0-390 for supporting the research project and 015MD0-089 for financial assistance with the postgraduate study.

NOMENCLATURE

A', B, B'	constants
A	surface area, m^2
G	volumetric gas flow rate, m^3/s
F	F-factor, $(kg/m^3)^{1/2}$
K	empirical parameter for centrifugal term
Q	volumetric flow rate, m^3/s
Z	axial height of the RPB, m
a	effective interfacial area, m^2/m^3
d	wire diameter of wire mesh packing, mm
$\dot{m}$	mass rate of flow, kg/s
g	gravitational constant, 9.806 m/s^2
ΔP_{total}	total pressure drop, Pa
ΔP_t	turbulent pressure drop, Pa
ΔP_c	centrifugal pressure drop, Pa
ΔP_m	momentum pressure drop, Pa
P^{cal}	pressure drop from calculation, bar
P^{exp}	pressure drop from experiment, bar
r	radius, m
r_1	packing inner radius, m
r_2	packing outer radius, m
V_0	axial-average tangential velocity of gas, m/s
$\overline{V_r}$	axial-averaged interstitial velocity of gas, m/s
U	superficial velocity, m/s
U_0	characteristic flow rate per unit, m/s

GREEK LETTERS

ω	rotating speed, rpm
ε	porosity of packing, m^3/m^3
ϵ	liquid holdup (m^3/m^3)
ρ	density, kg/m^3
ρ_g	density of gas, kg/m^3
ρ_L	density of liquid, kg/m^3

ABBREVIATIONS

RPB	rotating packed bed
rpm	rotational per minute
LNG	liquefied natural gas
R^2	correlation coefficients
AARD	average relative deviation

REFERENCES

(1) Yang, Z.; Sánchez-Ramírez, E.; Yang, A.; et al. Process intensification from conventional to advanced distillations: Past, present and future. *Chem. Eng. Res. Des.* **2022**, *188*, 378−392, DOI: 10.1016/j.cherd.2022.09.056.

(2) Kooijman, H. A.; Sorensen, E. Recent advances and future perspectives on more sustainable and energy efficient distillation processes. *Chem. Eng. Res. Des.* **2022**, *188*, 473−482, DOI: 10.1016/j.cherd.2022.10.005.

(3) Blahušiak, M.; Kiss, A. A.; Kersten, S. R. A.; Schuur, B. Quick assessment of binary distillation efficiency using a heat engine perspective. *Energy* **2016**, *116*, 20−31.

(4) Ramshaw, C.; Mallinson, R. H. Mass Transfer Process. U.S. Patent US4,283,255, 1981.
(5) Chen, J.-F.; et al. Cationic polymerization in rotating packed bed reactor: Experimental and modeling. *AIChE J.* **2010**, *56*, 1053−1062, DOI: 10.1002/aic.11911.
(6) Zhang, L.-L.; et al. Efficient Capture of Carbon Dioxide with Novel Mass-Transfer Intensification Device Using Ionic Liquids. *AIChE J.* **2013**, *59*, 2957−2965, DOI: 10.1002/aic.14072.
(7) Luo, Y.; Luo, J.; Chu, G.; Zhao, Z.; Arowo, M. Investigation of effective interfacial area in a rotating packed bed with structured stainless steel wire mesh packing. *Chem. Eng. Sci.* **2017**, *170*, 347−354, DOI: 10.1016/j.ces.2016.10.023.
(8) Alatyar, A. M.; Berrouk, A. S.; Alshehhi, M. S.; et al. Design optimization of a rotating packed bed based on dry hydraulic performance. *Alexandria Eng. J.* **2023**, *70*, 475−493.
(9) Zhao, Z.; Wang, J.; Sun, B.; Arowo, M.; Shao, L. Mass transfer study of water deoxygenation in a rotor−stator reactor based on principal component regression method. *Chem. Eng. Res. Des.* **2018**, *132*, 677−685.
(10) Yuan, S.; Liu, Z.; Liu, G. High-gravity deoxygenation of jet fuels using rotating packed bed. *Fuel* **2022**, *314*, No. 123080, DOI: 10.1016/j.fuel.2021.123080.
(11) Li, W.; Wu, X.; Jiao, W.; Qi, G.; Liu, Y. Modelling of dust removal in rotating packed bed using artificial neural networks (ANN). *Appl. Therm. Eng.* **2017**, *112*, 208−213.
(12) Qian, Z.; Xu, L.; Li, Z. H.; Li, H.; Guo, K. Selective absorption of H2S from a gas mixture with CO 2 by aqueous N -methyldiethanolamine in a rotating packed bed. *Ind. Eng. Chem. Res.* **2010**, *49*, 6196−6203.
(13) Chen, T. L.; Chen, Y. H.; Chiang, P. C. Enhanced performance on simultaneous removal of NOx-SO2-CO2 using a high-gravity rotating packed bed and alkaline wastes towards green process intensification. *Chem. Eng. J.* **2020**, *393*, No. 124678.
(14) Li, Y.; Liu, Y.; Zhang, L.; Su, Q.; Jin, G. Absorption of NOx into nitric acid solution in rotating packed bed. *Chin. J. Chem. Eng.* **2010**, *18*, 244−248.
(15) Surmi, A.; Shariff, A. M.; Sow, S.; Lock, M. Modeling of Nitrogen Removal from Natural Gas in Rotating Packed Bed Using Artificial Neural Networks. *Molecules* **2023**, *28*, No. 5333, DOI: 10.3390/molecules28145333.
(16) Li, X.; Liu, Y.; Li, Z.; Wang, X. Continuous Distillation Experiment with Rotating Packed Bed. *Chin. J. Chem. Eng.* **2008**, *16*, 656−662.
(17) Hilpert, M.; Aranda, G. U. C.; Repke, J. U. Experimental analysis and rate-based stage modeling of multicomponent distillation in a Rotating Packed Bed. *Chem. Eng. Processes: Process Intensif.* **2022**, *171*, No. 108651, DOI: 10.1016/j.cep.2021.108651.
(18) Li, W.; Song, B.; Li, X.; Liu, Y. Modelling of vacuum distillation in a rotating packed bed by Aspen. *Appl. Therm. Eng.* **2017**, *117*, 322−329.
(19) Mondal, A.; Pramanik, A.; Bhowal, A.; Datta, S. Distillation studies in rotating packed bed with split packing. *Chem. Eng. Res. Des.* **2012**, *90*, 453−457.
(20) Chen, J. F.; Shao, L. Recent advances in nanoparticles production by high gravity technology - From fundamentals to commercialization. *J. Chem. Eng. Jpn.* **2007**, *40*, 896−904.
(21) Noeres, C.; Kenig, E. Y.; Górak, A. Modelling of reactive separation processes: Reactive absorption and reactive distillation. *Chem. Eng. Processes* **2003**, *42*, 157−178.
(22) Yuan, M. H.; Chen, Y. H.; Tsai, J. Y.; Chang, C. Y. Ammonia removal from ammonia-rich wastewater by air stripping using a rotating packed bed. *Process Saf. Environ. Prot.* **2016**, *102*, 777−785.
(23) Li, W.; Shi, X.; Zhang, S.; Qi, G. Modelling of ammonia recovery from wastewater by air stripping in rotating packed beds. *Sci. Total Environ.* **2020**, *702*, No. 134971.
(24) Jiao, W.; Luo, S.; He, Z.; Liu, Y. Applications of high gravity technologies for wastewater treatment: A review. *Chem. Eng. J.* **2017**, *313*, 912−927.
(25) Cheng, H.; Scott, K. An empirical model approach to gas e v olution reactions in a centrifugal field. *J. Electroanal. Chem.* **2003**, *544*, 75−85, DOI: 10.1016/S0022-0728(03)00078-0.
(26) Wang, M.-Y.; et al. Investigation of Chlor-Alkali Electrolysis Intensified by Super Gravity. *Acta Phys.−Chim. Sin.* **2008**, *24*, 520−526, DOI: 10.3866/PKU.WHXB20080330.
(27) Jiao, W.; Luo, S.; He, Z.; Liu, Y. Applications of high gravity technologies for wastewater treatment: A review. *Chem. Eng. J.* **2017**, *313*, 912−927, DOI: 10.1016/j.cej.2016.10.125.
(28) Shukla, C.; Mishra, P.; Dash, S. K. A review of process intensified CO2 capture in RPB for sustainability and contribution to industrial net zero. *Front. Energy Res.* **2023**, *11*, No. 1135188, DOI: 10.3389/fenrg.2023.1135188.
(29) Hefzi, M.; Shirzadi, M.; Abolhasani, M. Intensification of CO2 Capture by Monoethanolamine Solution in a Rotating Packed Bed Reactor Equipped with High Frequency Ultrasonic Transducers. *J. Heat Mass Transfer Res.* **2023**, *9*, 121−128, DOI: 10.22075/JHMTR.2023.27119.1379.
(30) Zahir, A.et al. Parametric Study of Experimental and CFD Simulation Based Hydrodynamics and Mass Transfer of Rotating Packed Bed: A Review. In *Archives of Computational Methods in Engineering*; Springer: Netherlands, 2023.
(31) Joel, A. S.; Wang, M.; Ramshaw, C.; Oko, E. Modelling, simulation and analysis of intensified regenerator for solvent based carbon capture using rotating packed bed technology. *Appl. Energy* **2017**, *203*, 11−25.
(32) Keyvani, M.; Gardner, N. C. Operating characteristics of rotating beds. *Chem. Eng. Prog.* **1988**, *85*, No. e1, DOI: 10.2172/7279454.
(33) Lin, C.; Chen, Y.; Liu, H. Prediction Oof Liquid Holdup in Countercurrent-Flow Rotating Packed Bed, vol. 78, April 2000, DOI: 10.1205/026387600527293.
(34) Jiao, W. Z.; Liu, Y. Z.; Qi, G. S. Gas Pressure Drop and Mass Transfer Characteristics in a Cross-flow Rotating Packed Bed with Porous Plate Packing. *Ind. Eng. Chem. Res.* **2010**, *49*, 3732−3740.
(35) Hendry, J. R.; Lee, J. G. M.; Attidekou, P. S. Pressure drop and flooding in rotating packed beds. *Chem. Eng. Processes: Process Intensif.* **2020**, *151*, No. 107908.
(36) Pyka, T.; Koop, J.; Held, C.; Schembecker, G. Dry Pressure Drop in a Two-Rotor Rotating Packed Bed. *Ind. Eng. Chem. Res.* **2022**, *61*, 17156−17165.
(37) Llerena-Chavez, H.; Larachi, F. Analysis of flow in rotating packed beds via CFD simulations-Dry pressure drop and gas flow maldistribution. *Chem. Eng. Sci.* **2009**, *64*, 2113−2126.
(38) Wojtasik-Malinowska, J.; Jaskulski, M.; Jaskulski, M. CFD simulation of gas pressure drop in porous packing for rotating packed beds (RPB) CO2 absorbers. *Environ. Sci. Pollut. Res.* **2022**, *29*, 71857−71870.
(39) Burns, J. R.; Jamil, J. N.; Ramshaw, C. Process intensification: Operating characteristics of rotating packed beds - determination of liquid hold-up for a high-voidage structured packing. *Chem. Eng. Sci.* **2000**, *55*, 2401−2415.
(40) Tang, Z.; et al. Process Intensification: Continuous Synthesis of Nitrosyl Sulfuric Acid in a Rotating Packed Bed Reactor. *Ind. Eng. Chem. Res.* **2023**, *62*, 17194 DOI: 10.1021/acs.iecr.3c01453.
(41) Pyka, T.; et al. Distributor Effects on Liquid Hold-Up in Rotating Packed Beds. *Ind. Eng. Chem. Res.* **2024**, *63*, 2000−2010, DOI: 10.1021/acs.iecr.3c03996.
(42) Wang, Y.-h.; Li, Y. m.; Lou, K. j.; et al. Improved Mass-Transfer Model for Distillation in a Pilot-Scale Concentric Ring Rotating Bed as a Rotating Packed Bed. *Ind. Eng. Chem. Res.* **2024**, *63*, 5984−5994, DOI: 10.1021/acs.iecr.3c03710.
(43) Sandilya, P.; Rao, D. P.; Sharma, A.; Biswas, G. Gas-phase mass transfer in a centrifugal contactor. *Ind. Eng. Chem. Res.* **2001**, *40*, 384−392.
(44) Lashkarbolooki, M. A General Model for Pressure Drop Prediction Across a Rotating Packed Bed. *Sep. Sci. Technol.* **2017**, *52*, 1843−1851, DOI: 10.1080/01496395.2017.1302476.

(45) Kelleher, T.; Fair, J. R. Distillation Studies in a High-Gravity Contactor. *Ind. Eng. Chem. Res.* **1996**, *35*, 4646−4655.
(46) Singh, S. P. Air Stripping of Volatile Organic Compounds from Groundwater:An Evaluation of a Centrifugal Vapor-Liquid Contactor, Doctoral Dissertation; University of Tennessee: Knoxville, 1989.
(47) Li, Y.; Lu, Y.; Wang, G.; et al. Liquid entrainment and flooding in a rotating zigzag bed. *Ind. Eng. Chem. Res.* **2015**, *54*, 2554−2563.
(48) Lin, C.-C.; Chen, Y.; Liu, H. Prediction of Liquid Holdup in Countercurrent-Flow Rotating Packed Bed. *Chem. Eng. Res. Des.* **2000**, *78*, 397−403, DOI: 10.1205/026387600527293.
(49) Qammar, H.; Hecht, F.; Skiborowski, M.; Górak, A. Experimental investigation and design of rotating packed beds for distillation. *Chem. Eng. Trans.* **2018**, *69*, 655−660, DOI: 10.3303/CET1869110.

https://doi.org/10.1021/acsomega.4c01128
ACS Omega 2024, 9, 28105−28113